

Color Model Analysis for Solder Pad Segmentation on Printed Circuit Boards

C.L.S.C Fonseka, Prof. J.A.K.S Jayasinghe

Department of Electronic & Telecommunication,
University of Moratuwa,
Sri Lanka.
ee05sameera@gmail.com, jaks@ent.mrt.ac.lk

Abstract—This paper presents and discuss the robustness and suitability of major color models that are extensively used in image processing applications, for the segmentation of solder joints on different printed circuit board (PCB) surfaces with the use of efficient color image segmentation techniques. A detailed analysis has been carried out with respect to the parameters of color vectors that lie on the foreground (solder pad area) and background (PCB surface area) over major PCB surface variations and solder pad appearances. Even though many automatic optical inspection (AOI) systems are available for the inspection of surface mount devices (SMD) with the use of prior teaching of individual component, no visual inspection system exists that performs the automatic identification and quality analysis of through hole technology (THT) joints. This paper completes the first stage of an AOI system for THT solder joint inspection with providing a suitable color model for solder joint segmentation over a given PCB type.

Keywords – Printed Circuit Board, Through Hole Technology, Automatic Optical Inspection, HSV Color Model, HSI Color Model, YIQ Color Model, $YCbCr$, Color Model, RGB Color Model, K-Means Clustering, Color Quantization, OTSU Method, Region of Interest, Color image segmentation

I. INTRODUCTION

In most electronics manufacturing companies, hand soldering plays a major role in their production environment besides wave soldering for soldering through hole technology (THT) components [1]. Some THT components cannot be fed into wave soldering process as they might be damaged, due to their high temperature endurance limitations. Such temperature sensitive THT components are usually manually soldered. But the quality of manual soldering process heavily depends on the practical skills of the human operator. A THT soldering robotic system [2] with an integrated automatic optical inspection (AOI) [3], will overcome the issues related to human operators in manual soldering process and improves real time quality assurance of the system. Even though many brands of AOI systems from different vendors are available

for the inspection of surface mount devices (SMD), they require prior teaching to get accurate results. But for a THT joint soldering robotic system, this type of prior teaching of solder joints is not suitable as component lead directions may vary. Hence an AOI system that automatically identifies the solder joints with its lead directions is better suited for THT soldering robots. Automatic identification of solder joint with its lead direction is not an easy task due to the varying parameters of printed circuit boards (PCB) and solder pads. In this paper, a detailed analysis is presented for various PCB solder mask colors and solder pad types, in order to select the best color model for solder joint processing on a soldering robotic system.

II. COLOR MODEL ANALYSIS

Color is perceived by humans as a combination of tristimuli R (Red), G (Green) and B (Blue) which are usually called three primary colors. Video monitors and televisions display color images by modulating the intensity of RGB components at each pixel of the image. Even though the RGB model is suitable for color displays, it is not suitable for color image processing because of high correlation among R, G, B components [4]. Several different color models like HSV, HSI, YIQ, Ycc , Ohta, RGI, CMYK, XYZ, Lab, etc. are used in image processing applications, which can be derived using either linear or non linear transformations from RGB color space [4]. Selecting a best color model that suits for an image processing application is a challenging task.

Fig. 1 illustrates how RGB color model is represented in a three dimensional space while Fig. 2 and Fig. 3 illustrate the mapping of colors for HSV and HSI color models respectively.

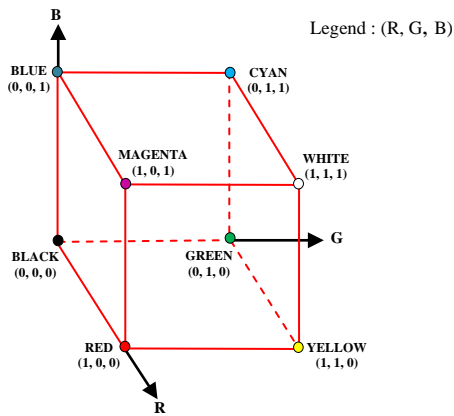


Fig. 1. RGB color model

HSV is a general purpose color model where color is represented in terms of hue (H), saturation (S) and brightness (V)[6, 25]. Transformation of RGB color model to HSV color model is carried out through Eq. 1, Eq. 2 and Eq. 3.

$$H = 60^\circ * H'(1)$$

$$S = \begin{cases} 0, & \text{if } C = 0 \\ \frac{C}{M}, & \text{if } C \neq 0 \end{cases} \quad (2)$$

$$V = M(3)$$

Where,

$$H' = \begin{cases} 0^\circ, & \text{if } C = 0 \\ \frac{(G - B)}{C} \text{ mod } 6, & \text{if } M = R \\ \frac{(B - R)}{C} + 2, & \text{if } M = G \\ \frac{(R - G)}{C} + 4, & \text{if } M = B \end{cases}$$

$$M = \max\{R, G, B\}$$

$$m = \min\{R, G, B\}$$

$$C = M - m$$

In the HSV color model hue (H) is expressed as an angle from 0° to 360° . Hue of red, yellow, green, cyan, blue and magenta is represented as $0^\circ, 60^\circ, 120^\circ, 180^\circ, 240^\circ$ and 300° respectively [5]. Saturation (S) is the depth or purity of the color which is represented as the distance from the vertical axis. Distance along the vertical axis represents the brightness value (V).

HSI is another general purpose color model where color is represented in terms of hue (H), saturation (S) and intensity (I). Transformation of RGB color model to HSI color model is carried out through Eq. 4, Eq. 5 and Eq. 6.

$$H = \cos^{-1} \left(\frac{(R - G) + (R - B)}{\sqrt{(R - G)^2 + (R - B)(G - B)}} \right) \quad (4)$$

$$S = 1 - \frac{3 \min(R, G, B)}{I} \quad (5)$$

$$I = \frac{(R + G + B)}{3} \quad (6)$$

Similar to HSV model, in the HSI color model hue (H) is also expressed as an angle from 0° to 360° . Hue of red, yellow, green, cyan, blue and magenta is represented as $0^\circ, 60^\circ, 120^\circ, 180^\circ, 240^\circ$ and 300° respectively. Saturation (S) is represented as the distance from the vertical axis and distance along the vertical axis represents the intensity value (I).

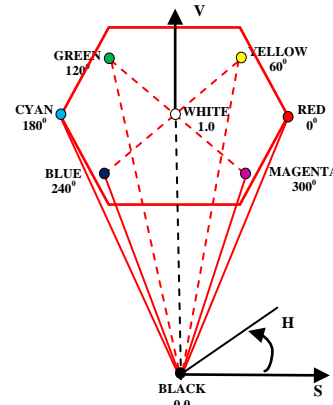


Fig. 2. HSV color model

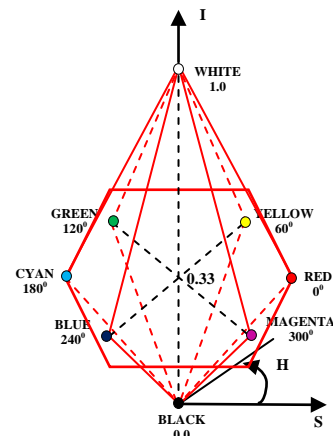


Fig. 3. HSI color model

From Fig. 01 to Fig. 03, it can be observed that colors are mapped to different points in 3-D Cartesian coordinate system by applying HSV and HSI color transformation. For an example, in the original RGB model, yellow color is represented by coordinate (0, 1, 0) and blue color is represented by coordinate (0, 0, 1). The vector length between these two colors is $\sqrt{3}$. In HSV model, yellow and blue color is represented by coordinates (60, 1, 1) and (240, 1, 1) respectively. The vector length between these two colors in HSV model is 2, which is larger than the vector length in the original RGB model. Further in the HSI model, yellow and blue color is represented by coordinates (60, 1, 0.33) and (240, 1, 0.33) respectively. The vector length between these two colors in HSV model is 2. Effectiveness of extraction of certain color features of an image can be improved by maximizing the vector length. Hence color transformation plays an important role in extracting features of a color image. There are many more

color transformations such as YIQ, YCbCr, I1I2I3, XYZ, Lab and etc.

YIQ is the color model used to encode color information in TV signal for NTSC TV system and it is intended to take advantage of human color-response characteristics[7]. Transformation of RGB color model to YIQ color model is carried out through Eq. (7), Eq. (8) and Eq. (9).

$$Y = 0.299 * R + 0.587 * G + 0.114 * B \quad (7)$$

$$I = 0.596 * R - 0.275 * G - 0.321 * B \quad (8)$$

$$Q = 0.212 * R - 0.523 * G + 0.311 * B \quad (9)$$

The Y component, is a measure of the luminance of the color, and is a likely candidate for edge detection in a color image while I and Q components describe the hue and saturation of the image[4].

YCbCr Model is used as a part of the color image pipeline in video and digital photography systems. Transformation of RGB color model to YCbCr color model is carried out through Eq. (10), Eq. (11) and Eq. (12).

$$Y = 0.299 * R + 0.587 * G + 0.114 * B \quad (10)$$

$$C_b = -0.169 * R - 0.331 * G + 0.5 * B \quad (11)$$

$$C_r = 0.5 * R - 0.419 * G - 0.081 * B \quad (12)$$

The Y component is the luma component and Cb and Cr are the blue difference and red difference chroma components [8].

I1I2I3 is another linear color transformation from RGB space used in image segmentation applications [4]. Transformation of RGB color model to I1I2I3 color model is carried out through Eq. (13), Eq. (14) and Eq. (15).

$$I1 = (R + G + B)/3 \quad (13)$$

$$I2 = (R - B)/2 \quad (14)$$

$$I3 = (2 * G - R - B)/4 \quad (15)$$

Tz-Sheng Peng and Chiou-Shann Fuh described that modified version of I1I2I3 color space rendered better results for solder joint segmentation among other models [9]. Transformation of RGB color model to modified I1I2I3 color model is carried out through Eq. (16), Eq. (17) and Eq. (18).

$$CH0 = (R + G + B)/3 \quad (16)$$

$$CH1 = (R - B) \quad (17)$$

$$CH2 = (2 * G - R - B) \quad (18)$$

XYZ color model, which is one of the most important color spaces defined by the international commission on illumination (CIE) [28]. This color space is the most common way in technical colorimetric work to describe the color of light [28]. Transformation of RGB color model to XYZ color model is carried out through Eq. (19).

$$\begin{bmatrix} X \\ Y \\ Z \end{bmatrix} = [M] \begin{bmatrix} R \\ G \\ B \end{bmatrix} \quad (19)$$

Where,

$$[M] = \begin{bmatrix} S_r X_r & S_g X_g & S_b X_b \\ S_r Y_r & S_g Y_g & S_b Y_b \\ S_r Z_r & S_g Z_g & S_b Z_b \end{bmatrix}$$

$$X_r = \frac{x_r}{y_r}$$

$$Y_r = 1$$

$$Z_r = (1 - x_r - y_r)/y_r$$

$$X_g = x_g/y_g$$

$$Y_g = 1$$

$$Z_g = (1 - x_g - y_g)/y_g$$

$$X_b = x_b/y_b$$

$$Y_b = 1$$

$$Z_b = (1 - x_b - y_b)/y_b$$

$$\begin{bmatrix} S_r \\ S_g \\ S_b \end{bmatrix} = \begin{bmatrix} X_r & X_g & X_b \\ Y_r & Y_g & Y_b \\ Z_r & Z_g & Z_b \end{bmatrix}^{-1} \begin{bmatrix} X_w \\ Y_w \\ Z_w \end{bmatrix}$$

Here, (xr, yr), (xg, yg), (xb, yb) are the chromacity coordinates of a given RGB system and (Xw, Yw, Zw) are the reference white of these coordinates.

Lab color space is designed to approximate human vision where color is represented in terms of lightness (L) while a and b components describe color component dimensions based on non linearly compressed coordinates [27]. This color space is useful for sharpening images and removing artifacts in images from digital cameras and scanners. Transformation of RGB color model to Lab color model is carried out through Eq. (20), Eq. (21) and Eq. (22).

$$L = 116 * f(Y/Y_n) - 16 \quad (20)$$

$$a = 500 [f(X/X_n) - f(Y/Y_n)] \quad (21)$$

$$b = 500 [f(Y/Y_n) - f(Z/Z_n)] \quad (22)$$

Where,

$$f(t) = \begin{cases} t^{1/3} & , \text{if } t > \left(\frac{6}{29}\right)^3 \\ \frac{1}{3} \left(\frac{29}{6}\right)^2 t + \frac{4}{29} & , \text{otherwise} \end{cases}$$

Here Xn, Yn and Zn are the CIE XYZ tristimulus values of the reference white point.

III. COLOR MODEL PERFORMANCE ANALYSIS

Eventhough these color models have been proven to render better results over many applications through out the years, their robustness, stability and accuracy must be verified with a mathematical approach for solder joint processing. Suitability of these color models for solder joint processing may vary due to the varying parameters of solder pads, PCB surface finish, PCB color, silk screen layer and etc. For accurate solder joint processing, a color model which maximize the vector distance between the solder pad area (foreground) and immediately surrounding PCB area (background) is better suited. Typical solder joint foreground and background for two different PCB types are shown in Fig. 4.

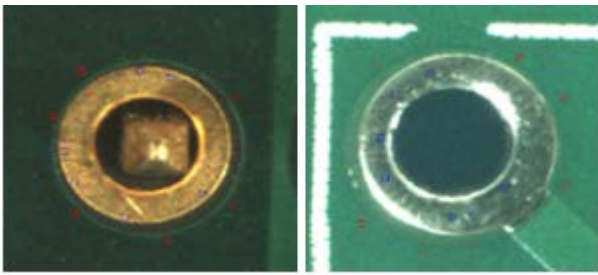


Fig. 4. Selected regions of a solder joint foreground and background

The average and the standard deviation of the vector distance between the foreground and background of following PCB solder mask colors and pad plating types were analyzed.

- Green PCBs with gold plated solder pads
- Green PCBs with tin plated solder pads
- Blue PCBs with gold plated solder pads
- Red PCBs with tin plated solder pads
- Black PCBs with tin plated solder pads

In this analysis process, background and foreground were carefully selected with minimum noise components. Table I to Table V illustrate the outcome of this data analysis process over these PCB types with nine different color models.

Table I. Data Analysis for Green PCB Gold Plated

Color Model	Average	Standard Deviation
RGB	165.661	20.856
HSV	134.112	17.888
HSI	127.008	29.525
YIQ	215.517	9.421
I ₁ I ₂ I ₃ Modified	128.44	17.005
YCbCr	105.945	13.079
XYZ	152.901	24.598
I ₁ I ₂ I ₃	168.663	26.008
Lab	120.852	14.240

Table II. Data Analysis for Blue PCB Gold Plated

Color Model	Average	Standard Deviation
RGB	179.962	30.359
HSV	144.076	11.775
HSI	134.966	17.714
YIQ	298.364	12.811
I ₁ I ₂ I ₃ Modified	154.298	12.926
YCbCr	131.388	14.995
XYZ	164.979	26.244
I ₁ I ₂ I ₃	170.256	16.235
Lab	126.580	16.221

Table III. Data Analysis for Green PCB Tin Plated

Color Model	Average	Standard Deviation
RGB	43.097	14.178
HSV	75.053	8.279
HSI	59.3	7.081
YIQ	27.901	5.331
I ₁ I ₂ I ₃ Modified	63.913	7.886
YCbCr	187.929	38.961
XYZ	25.386	16.915
I ₁ I ₂ I ₃	35.84	33.58
Lab	21.776	4.263

Table IV. Data Analysis for Red PCB Tin Plated

Color Model	Average	Standard Deviation
RGB	104.589	3.868
HSV	176.187	22.163
HSI	150.620	23.463
YIQ	74.644	3.0967
I ₁ I ₂ I ₃ Modified	63.439	6.217
YCbCr	56.369	3.131
XYZ	38.843	2.006
I ₁ I ₂ I ₃	62.759	26.469
Lab	61.287	1.306

Table V. Data Analysis for Black PCB Tin Plated

Color Model	Average	Standard Deviation
RGB	112.044	20.103
HSV	74.063	11.911
HSI	69.379	10.967
YIQ	76.991	8.900
I ₁ I ₂ I ₃ Modified	48.572	8.678
YCbCr	69.394	12.411
XYZ	108.563	20.320
I ₁ I ₂ I ₃	72.222	8.614
Lab	72.443	12.151

Eventhough Tz-Sheng Peng and Chiou-Shann Fuh described that modified I₁I₂I₃ model rendered much better results in solder joint segmentation [9], it is noted that other color models record higher average of vector length between foreground and background as observed in Table I to Table V. Fig. 5 illustrates the output of modified I₁I₂I₃ over these different PCB types.

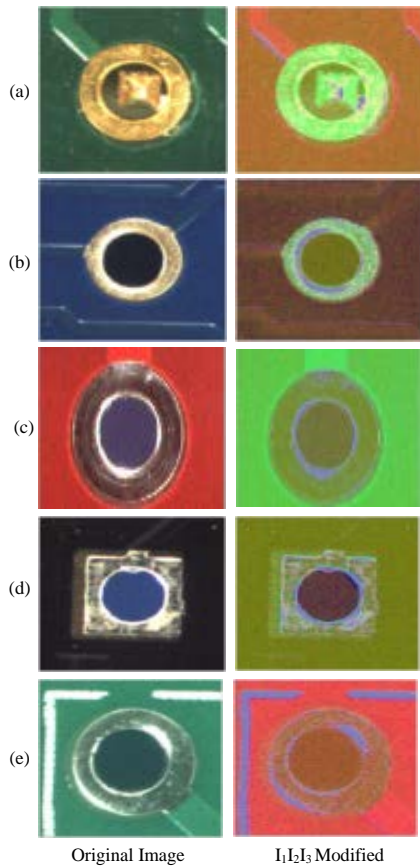


Fig. 5. (a) Green PCB-Gold Plated. (b) Blue PCB-Gold Plated. (c) Red PCB-Tin Plated. (d) Black PCB-Tin Plated. (e) Green PCB-Tin Plated

According to table I, YIQ color model gives an optimum result with a larger vector distance between foreground and background of a solder pad with a low standard deviation with respect to the other color models for green PCBs with gold plated solder pads. The Result originated from the YIQ color space can also be compared with color perception wheel which is illustrated in Fig. 6.



Fig. 6. Color perception wheel

It can be observed that the distance between the positions of background color and the foreground color of the YIQ transformed image is much wider comparing to other color models in the color wheel as illustrated in Fig. 11, that contains first four color models that give the maximum vector length difference between background and foreground. According to Fig. 7, it is clear that YIQ color

model provides less noise and distinct outcome for green color PCBs with gold plated solder pads.

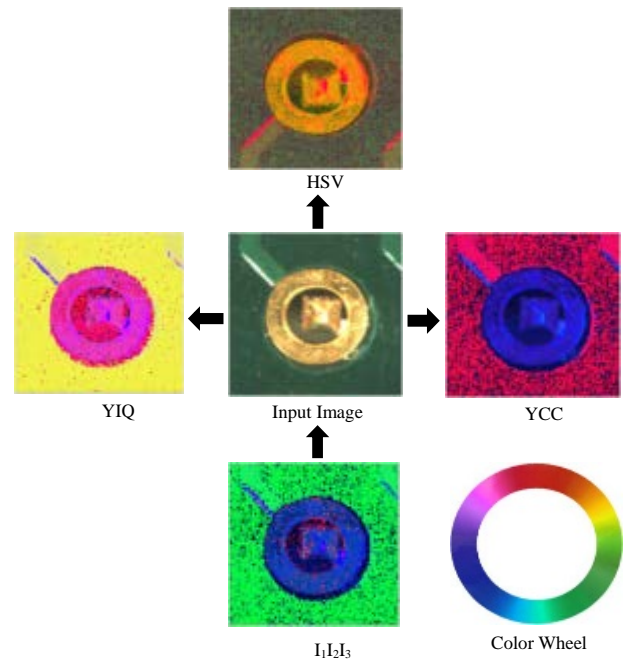


Fig. 7. Color space transformation of a gold plated solder joint on green PCB

Fig. 8 illustrates the YIQ color transformation over several solder pads.

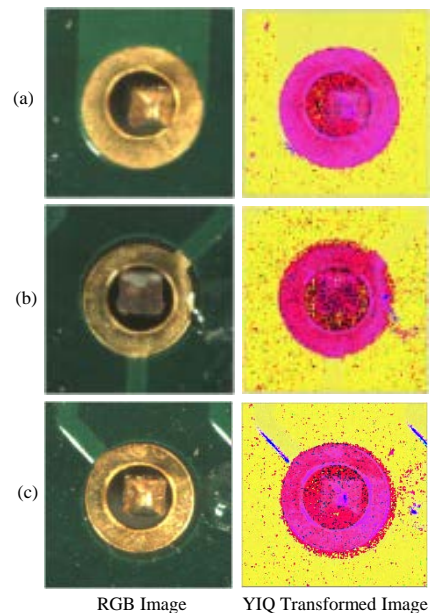


Fig. 8. (a) Gold plated solder joint placed on a different color path. (b) Gold plated solder joint with flux. (c) Gold plated solder joint with an illuminated PCB track.

YIQ color model is also capable of giving more robust and distinguishable outcome for blue PCBs with gold plated solder pads according to table II. The mapped colors of both foreground and background areas of the PCB, lie at almost opposite directions of the color wheel as illustrated in Fig. 9. Fig. 9 shows the first four color models that give the highest vector length difference for blue color PCB.

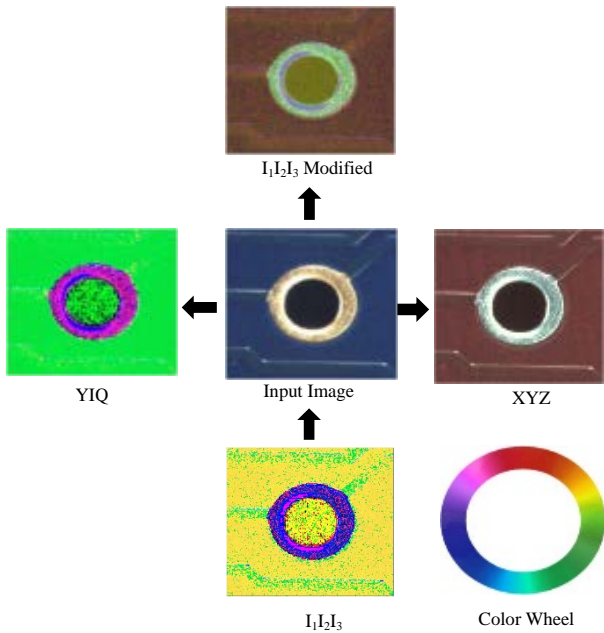


Fig. 9. Color space transformation of a gold plated solder joint on blue PCB.

Fig. 10 illustrates the outcome of YIQ color space over several solder pads on blue color PCB.

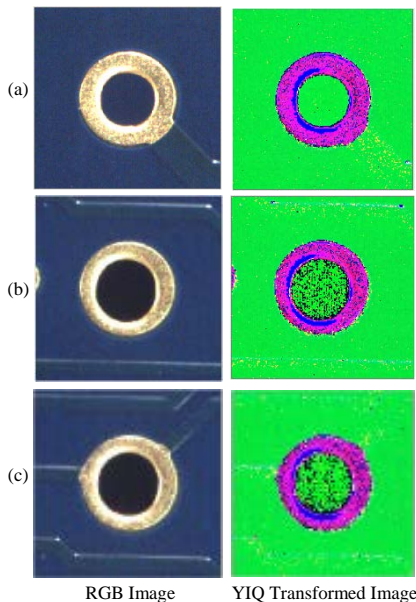


Fig. 10. (a) Gold plated solder joint with a PCB track. (b) Gold plated solder joint without a PCB track. (c) Gold plated solder joint with an illuminated PCB track

According to table III, none of the color models gives distinguishable vector length difference for Green PCB with tin plated solder pads, except YC_bC_r color space. The mapped colors lie at much wider distance of the color wheel when compared to other color models as illustrated in Fig. 11. This model provides more stable outcome even with larger standard deviation when comparing with other color

models over PCBs with tin plated solder pads on a green PCB. Fig. 11 illustrates the outcome of first four color models that give distinguishable results for tin plated solder pads.

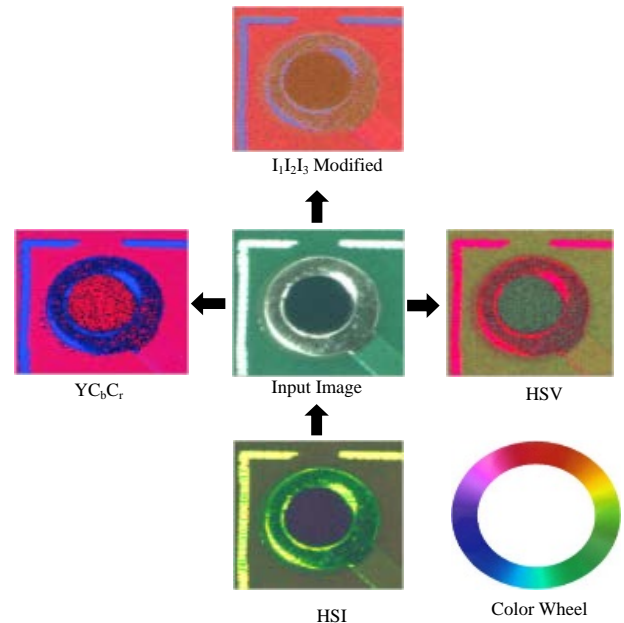


Fig. 11. Color space transformation of a tin plated solder joint on green PCB

Eventhough the transformed image consists of random noises on the object area, these noisy areas could be easily minimized with proper filtering on the image. Fig. 12 illustrates the results of YC_bC_r color transformation for several different tin plated solder joints on green color PCB.

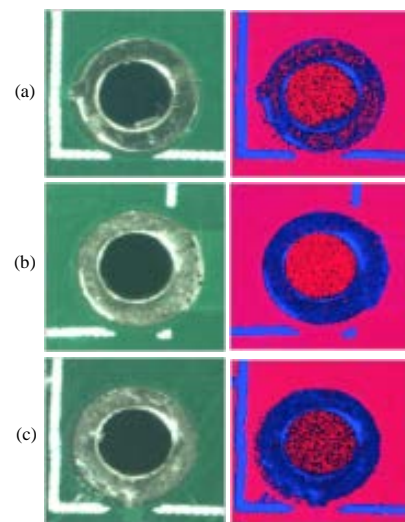


Fig. 12. (a) Tin plated solder joint with a silk screen marking closer to bottom margin of a solder pad. (b) Tin plated solder joint with a silk screen marking across a solder pad. (c) Tin plated solder joint with silk screen marking and small amount of flux closer to bottom margin of a solder pad.

According to table IV, HSV color model gives the best vector length difference between background and foreground for tin plated solder pads on a red color PCB. Fig 13

illustrates the results of color models for tin plated solder pad on a red color PCB. It can be observed that the mapped colors from this color transformation lie at almost opposite directions of the color perception wheel.

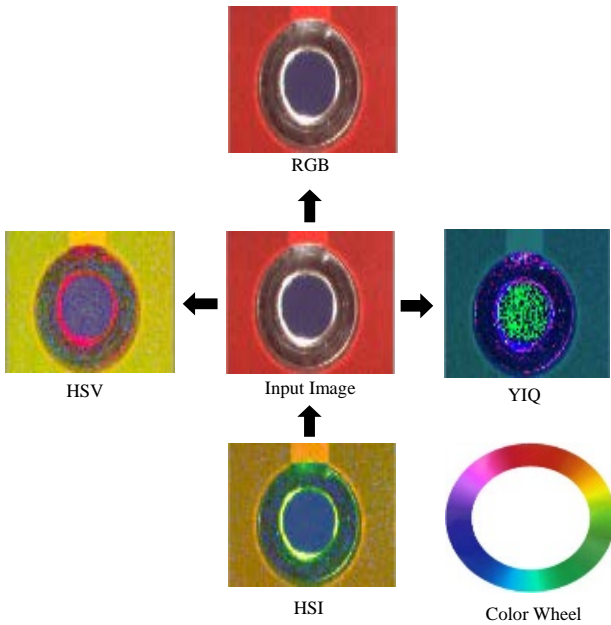


Fig. 13. Color space transformation of a tin plated solder joint on red PCB

Fig. 14 illustrates the result of this transformation over several tin plated solder joints on a red color PCB.

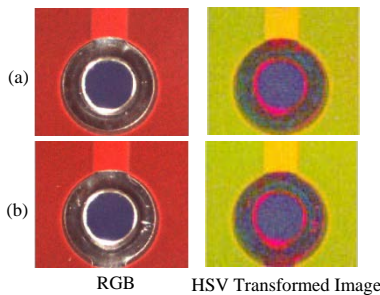


Fig. 14.(a) Tin plated solder joint on a red color PCB under less illuminated environment. (b) Tin plated solder joint on a red color PCB under illuminated environment.

According to table V, both RGB and XYZ color spaces provide approximately similar results on tin plated solder joints on a black color PCB. Fig. 15 illustrates the outcome of color models for a tin plated solder pad on a black PCB.

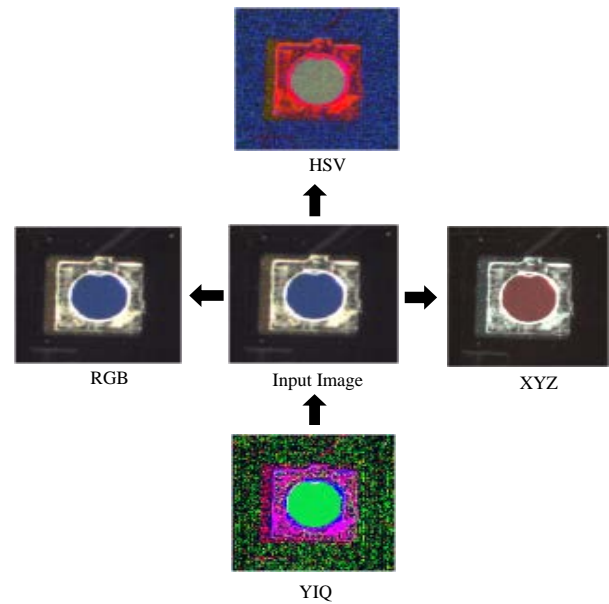


Fig. 15. Color space transformation of a tin plated solder joint on black PCB

Fig. 16 illustrates several tin plated solder joints acquired from an industrial imaging camera in RGB format on a black color PCB and their corresponding XYZ color transformation.

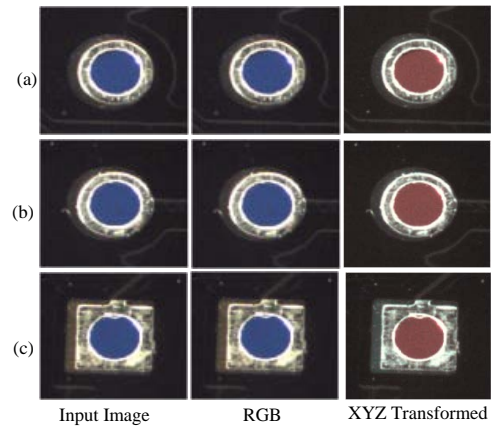


Fig. 16. (a) RGB image and corresponding XYZ transformed image of a tin plated solder joint without a track on black color PCB. (b) RGB image and corresponding XYZ transformed image of a tin plated solder joint with a track on black color PCB. (c) RGB image and corresponding XYZ transformed image of a tin plated solder joint with a shifted solder pad on black color PCB.

The selection of the color model as RGB or XYZ depends on the application requirement. In this study, the time that has to be spent on processing the image is one of the most critical parameters. Therefore RGB image will be taken as the processing model in this study to segment solder joint area of a black color PCB in order to save the processing time of the color space transformation.

IV. IMAGE TYPE VERIFICATION FOR IMAGE SEGMENTATION

Once the suitable color model is computed, next step is to decide the appropriate image type (color image or gray scale image) to perform image segmentation. Same analysis procedure is carried out on gray scale images on each channel of color models to compute the vector length difference between foreground and background. Table VI illustrates the parameters calculated for gray scale images on individual channels and color image for green PCBs with gold plated solder joints.

Table VI. Data Analysis for Green PCB Gold Plated

Color Model	CH0		CH1		CH2		Color Image	
	Av g	ST D	Av g	ST D	Av g	ST D	Av g	ST D
RGB	32.7	7.5	90.3	12.2	15.9	14.7	186	16.8
HSV	48.8	2.18	56.2	10.7	13.2	13.8	153	14
HSI	48.8	2.17	87	9.57	10.4	26.7	145	21.9
YIQ	10.5	10.5	19.1	6.97	7.71	7.87	218.3	7.49
I ₁ I ₂ I ₃ Mod.	70.6	7.01	12.0	10.6	15.6	12.7	140	11.8
YCbCr	10.4	10.5	13.4	2.34	99.2	46.6	148.5	32.9
XYZ	38.5	9.5	80.5	11.8	15.0	12.5	152.9	24.6
I ₁ I ₂ I ₃	10.8	11.8	35.6	11.3	85.1	25.1	172.3	27.3
Lab	40.5	21.8	65.8	12.9	70.5	17.8	120.8	14.2

According to Table VI, it is clear that color image processing is more appropriate than gray scale image processing for image segmentation, because gray scale images cannot even provide significant vector length difference even for gold plated solder joints where distinct background and foreground separation exists. Fig. 17 illustrates individual gray scale image on each channel of a gold plated solder joint on a green color PCB that has been transformed to YIQ color space.

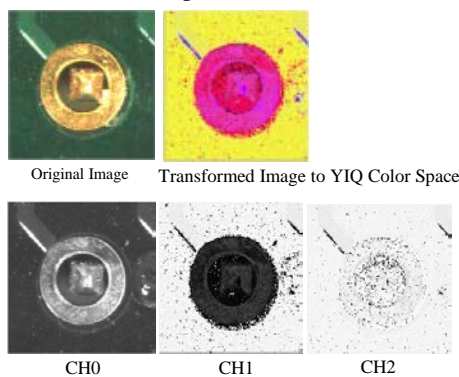


Fig. 17. Channels of YIQ color model

V. IMAGE SEGMENTATION

Image segmentation is considered as an important basic operation for meaningful analysis and interpretation of image acquired. It is one of the most critical and essential part of image analysis and one of the most difficult tasks in image processing, which determines the quality of final outcome of any image processing application. There is no unique image segmentation technique that can be applicable to each application. Many researches are extensively carried out in the field of color image processing, in order to find out more robust and adaptive algorithm for image segmentation. Recent works included variety of techniques: for example, stochastic model based approaches [10-11], morphological watershed based region growing [14], energy diffusion [15], graph partitioning [16], Quantitative evaluation methods [17], K-Means clustering [18], Fuzzy-C Means clustering [19] and etc.

The requirement of a color image segmentation algorithm that provides less computational complexity is much more important in this application to reduce the processing time on a solder joint. The analysis that has been carried out to find the color model that contains foreground and background color vectors lie at a maximum distance to each other, makes the segmentation task much more easier for a given PCB and solder pad, since it minimizes the no of iterations that should be made by the algorithm to to quantize colors. The color image segmentation algorithm, K-Means clustering has been chosen to detect solder pads in this application after taking above factors into consideration. Fig. 18 illustrates the proposed structure for segmenting a solder pad from its PCB background.

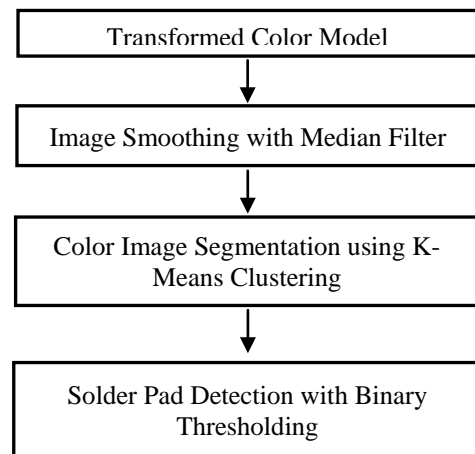


Fig. 18. Structure for Image Segmentation Process

For effective image segmentation, removal of noise while preserving the color boundaries is very important. Median filtering [20] is a non linear method and highly effective at removing noise while preserving edges with less computational overhead. The Median filter works by moving through the image pixel by pixel, while replacing each value with the median value of neighbouring pixels [20]. Fig. 19 illustrates the effect of median filter on different PCB images.

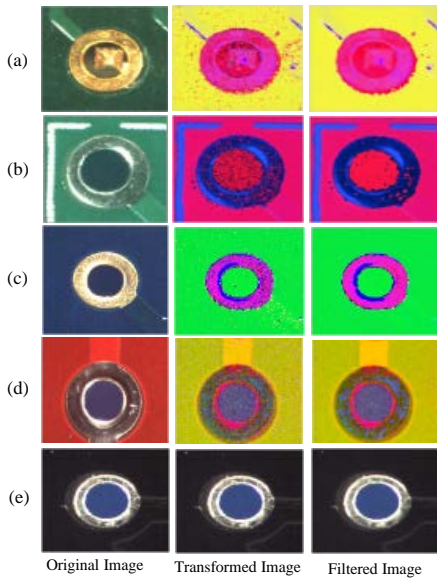


Fig. 19.(a) Output of median filter on gold plated solder pad on green PCB. (b) Output of median filter on tin plated solder pad on green PCB. (c) Output of median filter on gold plated solder pad on blue PCB. (d) Output of median filter on tin plated solder pad on red PCB. (e) Output of median filter on tin plated solder pad on black PCB.

The main step of image segmentation of a color image is to classify each pixel in a given image into one of a discrete number of color classes. In order to segment the image, colors in the image can be coarsely quantized to reduce the computational complexity. This can be effectively done with K-means algorithm [18], which is a vector quantization technique.

The main concept of K-Means clustering is to define K no of centres derived from a given data set, where each cluster contains group of elements that have the minimum distance to that particular centre [18]. In this segmentation process, only two centres are required that differentiate pixels lie on the foreground (solder pad) and background (PCB area). Algorithm randomly chooses two centroids C1 and C2 out of image data that possess the maximum vector length difference. Fig. 20 illustrates the selection of two centroids in a data set which have distributed color values over a limited range.

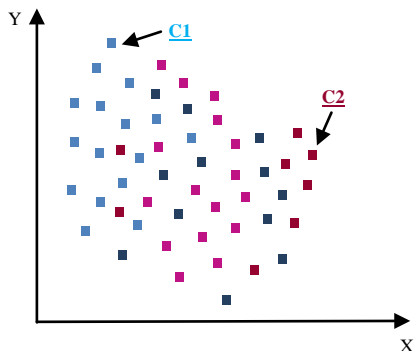


Fig. 20. Selection of centroid on a given data set

Then the distance from each point to both centroids is calculated and if the calculated distance is much closer to

C1, it is labelled as '1' and else it is labelled as '2'. Once the algorithm iterates through all the pixels in a given image, the two centroids are re-calculated based on the average color level within that particular cluster. Fig. 21 illustrates the outcome of this process.

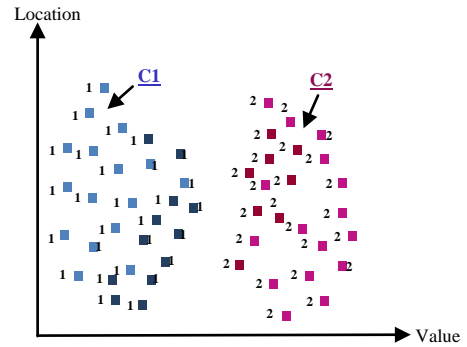


Fig. 21. Selection of centroid on a given data set

This process is iterated until both centroids are converged to fixed points. The final output value for these two centroids are such that sum of distance between each pixel value of the input image and their corresponding centroids are minimum. Fig. 22 illustrates the effect of this color segmentation algorithm on different PCB types.

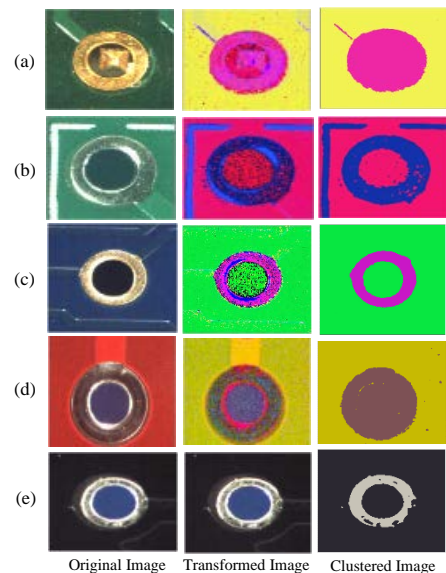


Fig. 22.(a) Output of k-means clustering on gold plated solder joint on green PCB. (b) Output of k-means clustering on tin plated solder joint on green PCB. (c) Output of k-means clustering on gold plated solder joint on blue PCB. (d) Output of k-means clustering on tin plated solder joint on red PCB. (e) Output of k-means clustering on tin plated solder joint on black PCB.

According to Fig. 22, it is obvious that the resulted image from K-Means clustering produces an output which has a minimum effect of uneven lighting, flux and other residuals on the PCB. Then the algorithm iterates through the image data to find out the color which contains the highest no of pixels. Then the image is thresholded according to Eq. 23.

$$P(x,y) = \begin{cases} 255, & \text{if } P(x,y) = M \\ 0, & \text{if } P(x,y) \neq M \end{cases} \quad (23)$$

M: Color that contains highest no of pixels

Fig. 21 illustrates the outcome of this algorithm over different PCB types.

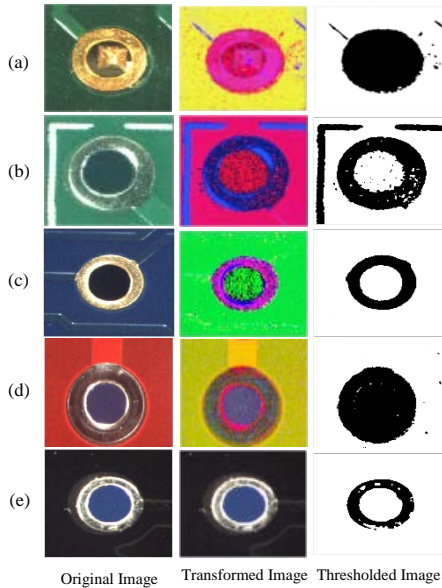


Fig. 21.(a) Thresholded gold plated solder joint on green PCB. (b) Thresholded tin plated solder joint on green PCB. (c) Thresholded gold plated solder joint on blue PCB. (d) Thresholded tin plated solder joint on red PCB. (e) Thresholded tin plated solder joint on black PCB.

Once the thresholding is done, the binary image is processed with morphological filtering [22, 23], in order to close open holes and reduce spread noise inside the resulted binary image. Then the contour finding algorithm [24], which is the method of identification of connected regions in an image, is used to segment discontinuous areas on the binary image. It iterates through all the connected regions and define a bounding rectangle that contains all the pixels belongs to that region. Then the system finds the largest and second largest regions of the detected contours in the image, because the area that possess by the solder pad should be contained by any of these two regions. After that the system finds the closest contour to the center point and the contour that lies much closer to one edge of the image. After that the solder joint area is computed depending on these results. Fig. 23 illustrates the detected solder joints over several images.

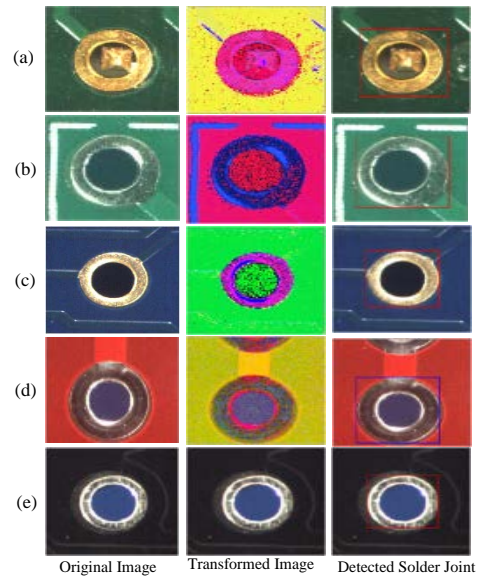


Fig. 23. (a) Detected gold plated solder joint on green PCB. (b) Detected tin plated solder joint on green PCB. (c) Detected gold plated solder joint on blue PCB. (d) Detected tin plated solder joint on red PCB. (e) Detected tin plated solder joint on black PCB.

The effectiveness of the color models that were selected through the analysis process and accuracy of the image segmentation algorithm must be verified with different conditions on different PCBs. Table VII summarizes the results obtained for different PCB types at different conditions. Each criteria contains 25 different samples taken at different conditions.

Table VII. Success Rate of Color Image Segmentation Process on Selected Color Models Over Different PCB Types at Different Controlled Conditions

PCB Type	Controlled Situation	YIQ	HSV	YCC	RGB
Gold Plated Solder Joint on Green Color PCB	Normal Condition (without any defect)	80%	100%	60%	100%
	Connected with PCB Track / Highly Illuminated	100%	96%	0%	100%
	Flux Applied	88%	96%	92%	96%
Gold Plated Solder Joint on Blue Color PCB	Normal Condition (without any defect)	100%	100%	72%	100%
	Connected with PCB Track / Highly Illuminated	72%	96%	72%	96%

	Flux Applied	68%	88%	88%	88%
Tin Plated Solder Joint on Green Color PCB	Normal Condition (without any defect)	16%	88%	100%	76%
	Connected with PCB Track / Higly Illuminate d	32%	100%	100%	20%
	Flux Applied	32%	80%	92%	72%
Tin Plated Solder Joint on Red Color PCB	Normal Condition (without any defect)	32%	100%	68%	82%
	Connected with PCB Track / Higly Illuminate d	32%	96%	20%	50%
	Flux Applied	0%	80%	60%	68%
Tin Plated Solder Joint on Black Color PCB	Normal Condition (without any defect)	16%	60%	96%	100%
	Connected with PCB Track / Higly Illuminate d	16%	56%	92%	100%
	Flux Applied	32%	40%	72%	80%

Manufacturing defects on the PCBs, like offsets between the drill hole pad and the plated pad area, lead to false detection of solder pads in YIQ color model for green color PCBs with gold plated solder pads as illustrated in Fig. 24.

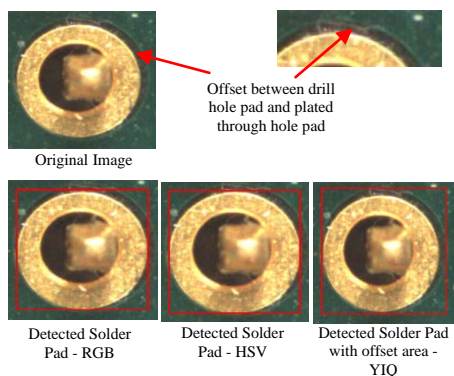


Fig. 24. Effect of offset issue on green color PCBs with gold plated solder pads.

Fig. 25 illustrates how this offset area influences the false detection of solder pad area during the image segmentation process.

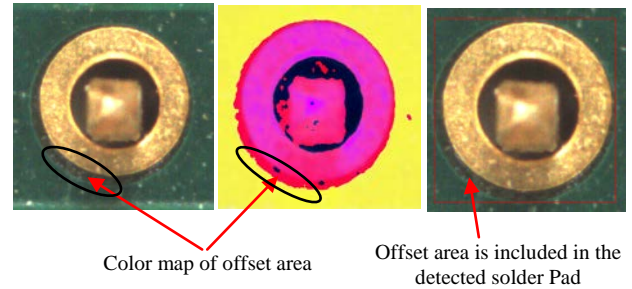


Fig. 25. Effect of offset issue on green color PCBs with gold plated solder pads.

According to Fig. 25, it can be observed that the offset area has been mapped to a color which has the minimum vector length difference to the color mapped for gold plated solder pad. Hence these two colors are mapped to a same color during color quantization process resulting a much larger object area detected during image segmentation process as illustrated in Fig. 25. In order to have an accurate detection of a solder pad area, this offset area must be carefully eliminated from solder pad.

Once the solder pad is detected including the offset area, segmented object is quantized to six different colors where the quantized colors include colors mapped for PCB background, solder pad, solder hole, offset area, highly illuminated areas due to uneven lighting and areas with different intensity levels on PCB background. Then the vector distances to each color vector was experimentally obtained over 100 gold plated solder pads on green color PCBs with reference to the origin of RGB color cube (0, 0, 0) as outlined in Table VIII.

Table VIII. Experimentally obtained color vector distances for quantized colors on the detected object area

Region of interest	Experimentally obtained vector distance range for different areas on the detected solder pad
Solder pad area	$285 \leq x \leq 330$
Offset area	$255 \leq x \leq 280$
Solder hole area	$0 \leq x \leq 100$
Background area	$350 \leq x \leq 370$

Here 'x' is referred to the calculated vector distance of a quantized color with reference to the origin of RGB color cube.

Then the algorithm iterates through all the pixels lie on the detected area and finds for the pixels whose vector distance falls in the calculated distance region of offset area as summarized in Table VIII. Then the particular pixel value is replaced by the color mapped for PCB background. Once this is done, color image segmentation process is repeated to locate the actual solder pad area from the detected object. Fig. 26 illustrates the outcome of this algorithm.

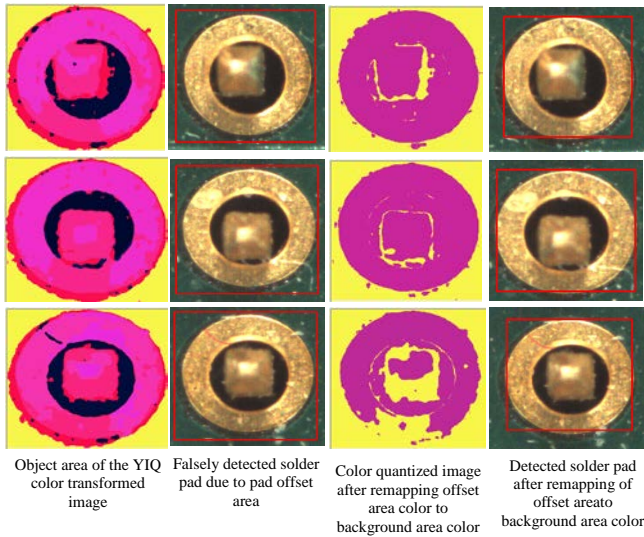


Fig. 26. Result of offset area removing algorithm.

In addition to the effect of offset area on gold plated solder pads on green color PCBs, the performance of the YIQ color model is considerably affected by gold plated solder pads with PCB tracks connected on blue color PCBs as illustrated in Fig. 27.

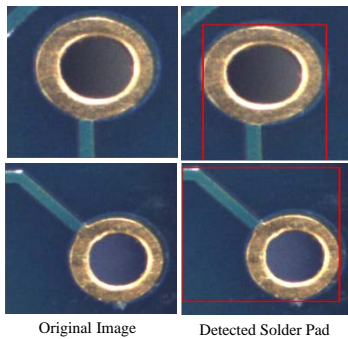


Fig. 27. False detection of solder pad areas due to light color PCB tracks on gold plated solder pads on blue color PCBs.

PCB tracks with light blue color are mapped to yellow color range during the color transformation from RGB to YIQ color space. The intensity of the mapped yellow color determines vector distances to mapped colors of PCB background and solder pad area. If the calculated distance from the color mapped for PCB track to the color mapped for solder pad is smaller comparing to the color mapped for PCB background, the PCB track color is mapped to a similar color as solder pad resulting a false identification of solder pad area. Fig. 28 illustrates how this effect has been taken place during color quantization process.

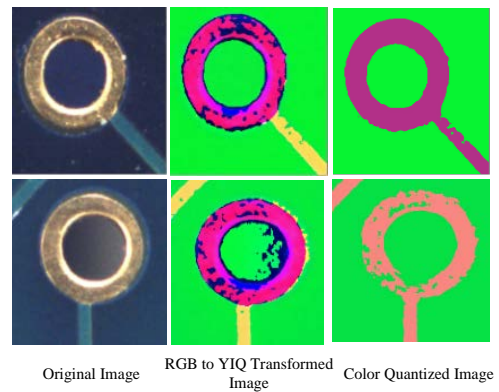


Fig. 28. Mapped colors during color transformation and color quantization processes for gold plated solder pads on blue color PCB.

The same procedure described earlier for eliminating pad offsets, is used to eliminate the effect of light color PCB tracks. Experimental results, obtained over 50 different solder pads with connected light color PCB tracks, show that the mapped color for PCB tracks lie in the vector distance range of 345 to 370 with reference to the origin of RGB color cube (0, 0, 0). Fig. 29 illustrates the outcome of developed algorithm over different solder pads with connected light color PCB tracks on blue color PCBs.

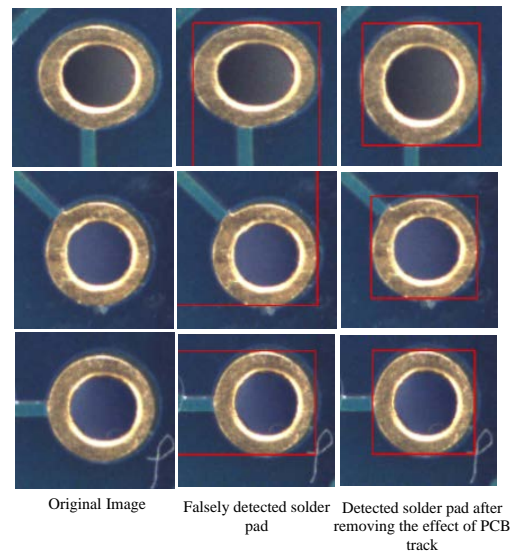


Fig. 29. Accurate detection of solder pads after removing the effect of PCB tracks on blue color PCBs with gold plated solder pads.

Table IX summarizes the success rate for YIQ color model after using the developed algorithm for removing the effect of pad offsets and light color PCB tracks.

Table IX. Hit rate after removing the effect of pad offsets and PCB tracks

PCB Type	Controlled Situation	Hit rate of YIQ color model before removing the effect of pad offsets & PCB tracks	Hit rate of YIQ color model after removing the effect of pad offsets & PCB tracks
Gold Plated Solder Joint on Green Color PCB	Normal Condition (without any defect)	90%	98%
	Connected with PCB Track / Higly Illuminated	100%	100%
	Flux Applied	88%	88%
Gold Plated Solder Joint on Blue Color PCB	Normal Condition (without any defect)	100%	100%
	Connected with PCB Track / Higly Illuminated	72%	100%
	Flux Applied	68%	80%

According to Table IX, it is clear that the new algorithm successfully eliminates the effect of manufacturing defects and surface finish of blue and gold color PCBs with gold plated solder pads much precisely.

Eventhough the modified color model from $I_1I_2I_3$ color space, was stated to provide better outcome for printed circuit board segmentation [11], we have shown that a single color model is not itself being capable of giving a more distinguishable image segmentation for different PCB colors with different solder pads according to the results obtained in this study.

VI. CONCLUSION

Eventhough the results obtained from this study fulfils the requirement of the automatic identification of solder pads on various PCB color types, these results will no longer give a stable and accurate detection rate once the solder pad is soldered from the robotic system. Once the soldering is completed, there will only be intensity variations of the solder paste color and PCB background color. Implementation of a new color model which will map the color of solder paste and PCB background will fulfile the requirement of the automatic detection of solder joint phase of the soldering robotic system.

REFERENCES

- [1] PCB Assembly Equipment for Through Hole Systems <http://www.ddmnavastar.com/through-hole-systems>
- [2] Gary Goldberg, "ROI of a Soldering Robot", Circuit Assembly Online Magazine, 26341-automation-1609.html
- [3] Eid M.Taha, E.Emary, Khalid Moustafa, "Automatic Optical Inspection for PCB Manufacturing : a survey", International Journal of scientific engineering & research, Volume 5, Issue 7, July 2014, ISSN 2229-5518
- [4] H.D Cheng, X.H Jiang, Y.Sun, Jing Li Wang, "Color Image Segmentation: Advances & Prospects"
- [5] Tinku Acharya, Ajoy K.Ray, "Image Processing Principles and Applications"
- [6] Adrian Ford, Alan Roberts, "Colour Space Conversions"
- [7] Baisa L.Gunjal, Suresh N.Mali, "Comparative Performance Analysis of DWT-SVD Based Color Image Watermarking Technique in YUV, RGB and YIQ Color Spaces"
- [8] Amanpreet Kaur, B.V Kranthi, "Comparison between YCbCr Color Space and CIE Lab Color Space for Skin Color Segmentation", International Journal of Applied Information Systems (IJ AIS) – ISSN : 2249-0868
- [9] Tz-Sheng Peng, Chiou-Shann Fuh "Color based printed circuit board solder segmentation", National Taiwan University.
- [10] James Bruce, Tucker Balch, Manuela Veloso, "Fast and Inexpensive Color Image Segmentation for Interactive Robots".
- [11] S. Belongie, et. al., "Color- and texture-based image segmentation using EM and its application to content-based imageretrieval", Proc. of ICCV, p. 675-82, 1998.
- [12] Y. Delignon, et. al., "Estimation of generalized mixtures and its application in image segmentation", IEEE Trans. on Image Processing, vol. 6, no. 10, p. 1364-76, 1997.
- [13] D.K. Panjwani and G. Healey, "Markov random field models for unsupervised segmentation of textured color images", PAMI, vol. 17, no. 10, p. 939-54, 1995.
- [14] L. Shafarenko, M. Petrou, and J. Kittler, "Automatic watershed segmentation of randomly textured color images", IEEE Trans. on Image Processing, vol. 6, no. 11, p. 1530-44, 1997.
- [15] W.Y. Ma and B.S. Manjunath, "Edge flow: a framework of boundary detection and image segmentation", Proc. of CVPR, pp 744-49, 1997.
- [16] J. Shi and J. Malik, "Normalized cuts and image segmentation", Proc. of CVPR, p. 731-37, 1997.
- [17] M. Borsotti, P. Campadelli, and R. Schettini, "Quantitative evaluation of color image segmentation results", Pattern Recognition letters, vol. 19, no. 8, p. 741-48, 1998.
- [18] Tapas Kanungo, Nathan S.Netanyahu, Christine D.Piatko, Ruth silverman, Angela Y.Wu, "An Efficient k-means clustering algorithm: analysis and implementation", IEEE transactions on pattern analysis and machine intelligence, Vol.24, No.7, july 2002
- [19] Sauma Dutta, Bidyut B. Chaudhuri, Fellow, "Homogenous Region based Color Image Segmentation", Proceedings of the World Congress on Engineering and Computer Science 2009 Vol II WCECS 2009, October 20-22, 2009, San Francisco, USA.
- [20] Sing hoong teoh, Boon tatt koik, Haidi Ibrahim, "Exploration of current trend on median filtering methods utilized in digital gray scale image processing", International journal of materials, mechanics and manufacturing, Vol.1, No.1, February 2013
- [21] Tz-Sheng Peng, Chiou-Shann Fuh "Color based printed circuit board solder segmentation", National Taiwan University.
- [22] Nang Seng Siri Mar, "Vision based classification of solder joint defects", Masters by Research, Queensland University of Technology, 2011.
- [23] Shao-Yi Chien, Liang-Gee-Chen, "Reconfigurable morphological image processing accelerator for video object segmentation", IEEE, 2008
- [24] estarch, "Learning image processing with OpenCV"
- [25] Harmeet kaul kelda, Prabheep kaur, "A Review: Color models in Image Processing", Int.J.Computer technology & applications, Vol 5(2), 319-322
- [26] Philippe colantoni, "Color SPace Transformations", University jean monnet.
- [27] Jean francois gonnet, "Colour effects of co-pigmentation of anthocyanins revisited—2.A colorimetric look at the solutions of

cyenin co-pigmented byrutin using the CIELAB scale”, Food chemistry 66 (3) : 387-394

[28] Douglas A.Kerr, “The CIE XYZ and xyY Color Spaces”, Issue 1, March 2010

AUTHORS

First Author – C.L.S.C Fonseka, Department of Electronic & Telecommunication, University of Moratuwa, Sri Lanka., Email: ee05sameera@gmail.com

Second Author – Prof.J.A.K.S Jayasinghe, Department of Electronic & Telecommunication, University of Moratuwa, Sri Lanka., Email: jaks@ent.mrt.ac.lk